batteries

MDPI

Article

Experimental Study on Fire Suppression of Lithium-Ion Battery Module with Different Extinguishing Agents in Confined Space

Yanbo Jia [1], Chaohui Shi [1], Lei Zhang [1], An Tao [1], Sen Hu [1] and Huang Li [2,*]

[1] Power China HuaDong Engineering Corporation Limited, Hangzhou 311122, China
[2] Institute of Advanced Technology, University of Science and Technology of China, Hefei 230000, China
* Correspondence: huangli@iat.ustc.edu.cn

Abstract

In order to investigate the suppression effect of different extinguishing agents on lithium-ion battery fires in real confined spaces, a comparative experiment was conducted using aerosols, heptafluoropropane, and perfluorohexanone. In tests without any fire suppression measures, the peak heat release rate reached up to 69.09 kW, and a total of 8.05 MJ of heat was generated along with multiple deflagration events. Moreover, the heptafluoropropane and perfluorohexanone both effectively extinguished the flames with extinguishing times of 12 and 20 s, respectively. The aerosol agent caused a significant contraction of the flames, but it was unable to achieve complete extinguishment. Regarding cooling performance, the heptafluoropropane decreased the front surface temperature of the battery by 147 °C, while perfluorohexanone achieved a reduction of 230 °C. Additionally, the liquid-phase adhesion characteristics of perfluorohexanone enabled sustained cooling. A comprehensive comparison indicates that the perfluorohexanone agent exhibits outstanding performance in flame extinguishment, cooling efficiency, and the suppression of thermal propagation. Heptafluoropropane demonstrates rapid fire suppression and is suitable as a fast-response agent, whereas the aerosol requires a multi-discharge design to achieve reliable performance. Based on these findings, it is recommended that energy storage systems adopt a composite suppression strategy for fire protection.

Keywords: lithium-ion battery; confined space; extinguishing agent; thermal runaway suppression; thermal propagation

1. Introduction

Lithium-ion batteries have become the core components of electric energy storage systems due to their advantages, such as their high energy density, long cycle life, and low self-discharge rate [1,2]. With the ongoing advancement of new energy strategies, the scale of the construction of energy storage power stations continues to expand, and the integration density of battery modules is increasing, leading to increasingly prominent fire safety hazards. Studies have indicated that lithium-ion batteries release large amounts of flammable gases under thermal runaway conditions, which may cause intense combustion or even explosions, therefore posing a serious threat to the safe operation of energy storage systems [3–6].

A confined space represents a typical operating environment for energy storage batteries within a battery pack. The sealed structure facilitates heat accumulation and hinders gas diffusion when a battery undergoes thermal runaway. And the flames can spread rapidly once the thermal runaway is triggered, making extinguishment difficult [7–10]. In

Check for updates

Academic Editor: Pascal Venet

Received: 11 May 2026
Revised: 6 June 2026
Accepted: 16 June 2026
Published: 25 June 2026

Copyright: © 2026 by the authors. Licensee MDPI, Basel, Switzerland. This article is an open access article distributed under the terms and conditions of the Creative Commons Attribution (CC BY) license.

recent years, researchers have conducted extensive studies on fire suppression in lithium-ion batteries. Extinguishing agents such as heptafluoropropane, perfluorohexanone, and aerosols are widely used for electrical fire prevention and control due to their good electrical insulation, minimal residues, and environmental friendliness [8–10]. In terms of mechanisms, researchers have explored the flame extinguishing and cooling characteristics of different agents [11–15]. For example, it was found that heptafluoropropane quickly extinguishes open flames but has limited cooling capability, while the liquid-phase adhesion characteristics of perfluorohexanone help delay thermal runaway propagation. However, existing studies are mostly conducted in open spaces or at the single-battery scale. Comparative research on the full evolution of battery pack fires in confined spaces and the comprehensive performance of various extinguishing agents remains relatively weak [14]. In particular, key issues such as the ability of extinguishing agents to suppress thermal propagation to adjacent cells, the interruption of heat transfer paths within the battery pack, and the coupling mechanisms of deflagration behavior in confined environments lack systematic evaluation.

With the purpose of investigating the effectiveness of common fire extinguishing agents in suppressing battery fires in practical application scenarios of energy storage systems. And the results can provide experimental evidence and theoretical support for the fire protection designs in energy storage systems. Furthermore, three typical extinguishing agents (aerosol, heptafluoropropane, and perfluorohexanone) are selected to conduct comparative fire suppression experiments on lithium-ion phosphate battery packs based on a full-scale fire simulation platform for lithium-ion battery energy storage systems. The comprehensive fire suppression performance of different agents in confined spaces is systematically evaluated by analyzing multiple indicators, including the open flame extinguishing time, cooling efficiency, heat release rate, and thermal propagation suppression capability.

2. Experiment

2.1. Experimental Platform

As shown in Figure 1, the experiments were conducted on a full-scale fire simulation platform for lithium-ion battery energy storage systems. The platform mainly includes a 10 MW calorimetry test system, a flue gas treatment system, a full-scale fire test site, and a 20-foot energy storage container. It is important to note that the 10 MW mentioned here denotes the heat release rate achieved during the combustion of substances, rather than indicating the capacity of the energy storage system.



Figure 1. Schematic of the full-scale fire simulation platform for lithium-ion battery energy storage systems.

The platform enables fire safety tests at multiple levels, including single cells, modules, battery clusters, and battery systems.

2.2. Experimental Setup

To simulate a real application scenario of energy storage batteries, this study used three 314 Ah lithium-ion phosphate batteries for energy storage. The specifications of the 314 Ah LFP are shown in Table 1.

Table 1. The specifications of the 314 Ah lithium-ion phosphate battery.

Series Number	MB31	Electrolyte	The Primary Is Lithium Hexafluorophosphate ($LiPF_6$)
Maximum charge/discharge current	157 A (0.5 P, 25 °C ± 2 °C)	Temperature range for normal operation	0~60 °C (charge) −20~60 °C (discharge)
Limited charge voltage	3.65 V	Cut-off discharge voltage	2.5 V (T > 0 °C); 2.0 V ($T \leq 0$ °C)
Nominal Capacity	3.2 V/314 Ah	Weight	5600 g ± 300 g

The arrangement of the fire suppression system inside the battery pack is one that is common energy storage systems, as shown in Figure 2. And the dimensions of this battery pack are 777 mm (width) ×1025 mm (length) × 230 mm (height).

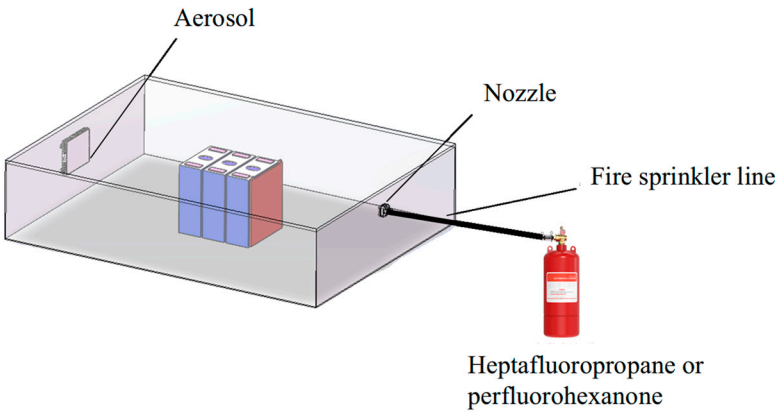


Figure 2. Schematic layout of fire suppression measures inside the battery pack.

During the experiments, thermal abuse was applied to Battery 1# using an constant heater to trigger thermal runaway. The electrical power of heater is set as 800 W refers to the standard GB36276 [16]. The heater was turned off once safety venting was observed. Moreover, the vented combustible gases were also ignited in order to observe the combustion behavior in four experimental cases: without an extinguishing agent, with the aerosol, with heptafluoropropane, and with perfluorohexanone (listed in Table 1).

As shown in Table 2, the nozzle coefficient was 2.0, while the diameter of the pipe leading from the extinguishing agent to the pack was 12 mm, which are common parameters used for fire extinguishing measures in energy storage systems.

Table 2. Experimental cases.

Experiment Number	Fire Extinguishing Agent	Nozzle Coefficient	Pipe Diameter	Amount of Extinguishing Agent
Test 1	Without the extinguishing agent	/	/	/
Test 2	Aerosol agent	/	/	30 g
Test 3	Heptafluoropropane agent	2.0	12 mm	3 kg
Test 4	Perfluorohexone agent	2.0	12 mm	3 kg

However, thermal runaway experiments still exhibit significant variability. Especially in confined spaces, the uncertainty of deflagration and re-ignition behaviors has a notable impact on the time required for fire extinguishment and the degree of temperature reduction, and this can also directly lead to differences in repeated experiments. Nevertheless, the critical blocking effects of different fire extinguishing agents on battery fire suppression and thermal diffusion can be clearly observed in this research.

With the aim of investigating the suppression efficacy of these general fire extinguishing agents on energy storage battery fires in real-life scenarios, the fire extinguishing measures were discharged roughly 1 min after confirming that the battery had entered a stable combustion stage. And the fire extinguishing agent will be expelled by the inert high-pressure gas that is pre-stored within the tank. Moreover, the predetermined dosage of the fire extinguishing agent was determined via calculations based on the dimensions of the experimental chamber, in accordance with standard GB50370 [17], as shown in Table 2.

2.3. Thermocouple Placement

As shown in Figure 3, temperatures on different surfaces of the batteries were collected. In this study, the surface close to the heating plate was defined as the front surface; the surface in contact with the adjacent battery was defined as the back surface; and the other two sides were defined as the side surfaces. The temperature measurement points are detailed in Table 3.

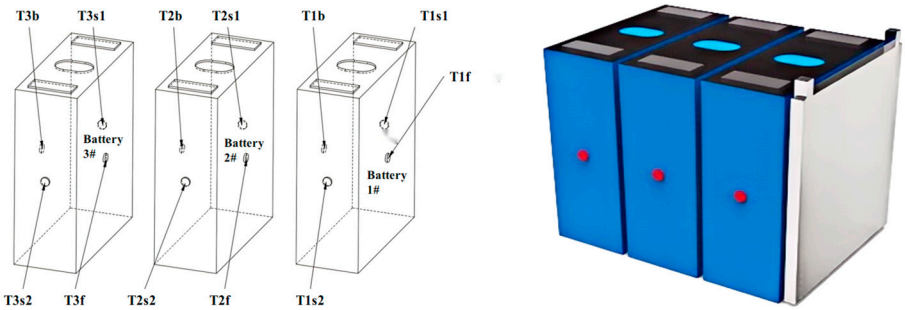


Figure 3. Experimental setup of the lithium-ion battery thermocouples.

Table 3. Measurement locations for different thermocouples.

Thermocouple	Location	Thermocouple	Location
T1f	Front wall of Battery 1#	T2s1	Side wall of Battery 2#
T1b	Back wall of Battery 1#	T2s2	Side wall of Battery 2#
T1s1	Side wall of Battery 1#	T3f	Front wall of Battery 3#
T1s2	Side wall of Battery 1#	T3b	Back wall of Battery 3#
T2f	Front wall of Battery 2#	T3s1	Side wall of Battery 3#
T2b	Front wall of Battery 2#	T3s2	Side wall of Battery 3#

3. Results

In this study, the fire suppression efficacy of various fire extinguishing agents in lithium-ion battery packs in energy storage systems was comprehensively evaluated through the comparative analysis of multiple parameters, including the open flame extinction time, cooling efficiency, heat release rate, and thermal diffusion inhibition capability.

Figure 4 illustrates the thermal runaway and fire behavior of a lithium-ion battery pack in the test without an extinguishing agent. According to relevant studies, the large volume of flammable gases released during lithium-ion phosphate battery thermal runaway readily undergo combustion and explosion upon mixing with air in confined conditions [3,6].

Compared to thermal runaway in open environments, the batteries in this study operated in a relatively sealed system, contacting external air through pressure relief vents while maintaining an internal air medium. Consequently, the mixture of the electrolyte vapor and flammable gases released by Battery 1# reacted with ambient air under sustained heat accumulation after the initial pressure relief, triggering a primary explosion at 2245 s. And no significant gas diffusion was observed externally after combustion due to the limited accumulation of explosive gases inside the container. As internal chemical reactions progressed, the gas generation rate increased progressively, leading to a secondary explosion at 3063 s. Following this secondary explosion, the thermal runaway intensified dramatically, producing substantial smoke emissions until it reached a stable combustion state at 3093 s, with the external flame completely extinguishing by 3242 s.

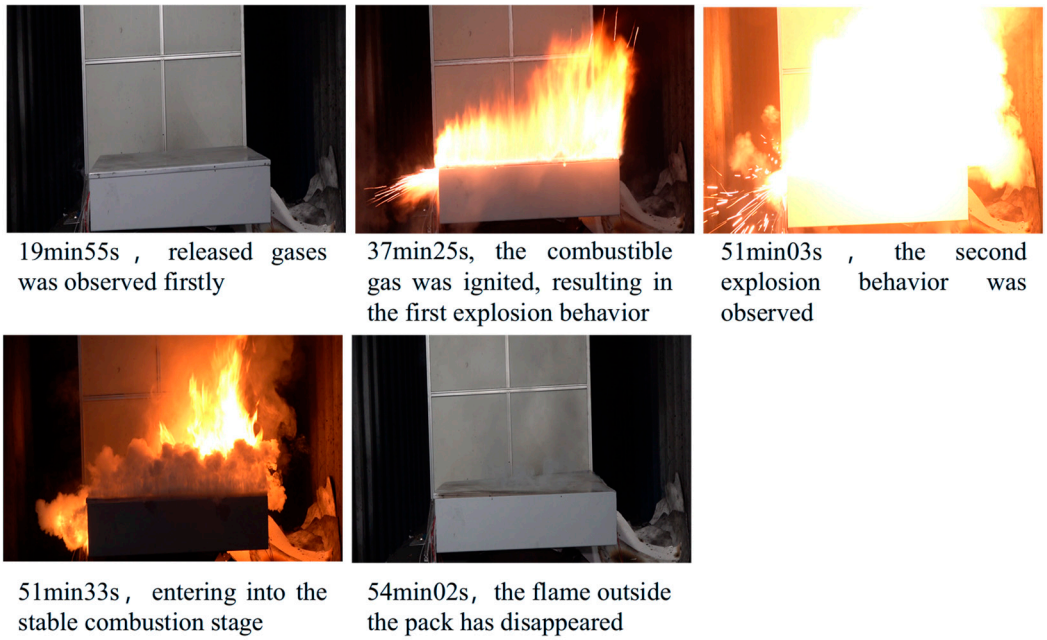


Figure 4. Thermal runaway and fire behavior of lithium-ion battery packs in the absence of fire suppression measures.

Figure 5 shows the curves of the thermal runaway temperature, voltage, and heat release rate for the lithium-ion battery pack in the test without an extinguishing agent. This process can be generally divided into three distinct stages based on the thermal runaway behavior of the battery.

Stage I: Lasting from 0 to 1195 s, this represents the heating-induced stage. During this period, the heating plate triggers chemical reactions within Battery 1#, causing the accumulation of combustible gases and electrolyte vapor inside the battery. At 1195 s, the safety valve of Battery 1# ruptures, allowing some gas to escape outside the pack. This rupture also releases hot gas, resulting in a slight temperature drop in Battery 1#, with T1f decreasing from 432.4 °C to 427.7 °C. Throughout this stage, the battery voltage (V1) remains stable without fluctuations. This demonstrates that in safety warning technologies in battery systems, the lagging of voltage warnings behind gas warnings must be considered.

Stage II: Lasting from 1196 to 3061 s, this represents the thermal runaway evolution stage of Battery 1#. During this period, chemical reactions persist within the battery as the temperature rises, and the acceleration of reaction rates also leads to a rapid increase in the gas release rate. Furthermore, the T1f reaches 497.1 °C at 3061 s, at which point the internal reaction rate exceeds the threshold, initiating the thermal runaway process characterized by a sharp temperature surge and an instantaneous voltage drop. Additionally, V1 drops from

3.5 V to 3.4 V at 1369 s during this stage, with similar behavior observed in Batteries 2# and 3#. The primary cause of this phenomenon is the detonation of the mixed gas, with a peak heat release rate of 16.0 kW and the total heat released during the detonation process amounting to 0.218 MJ.

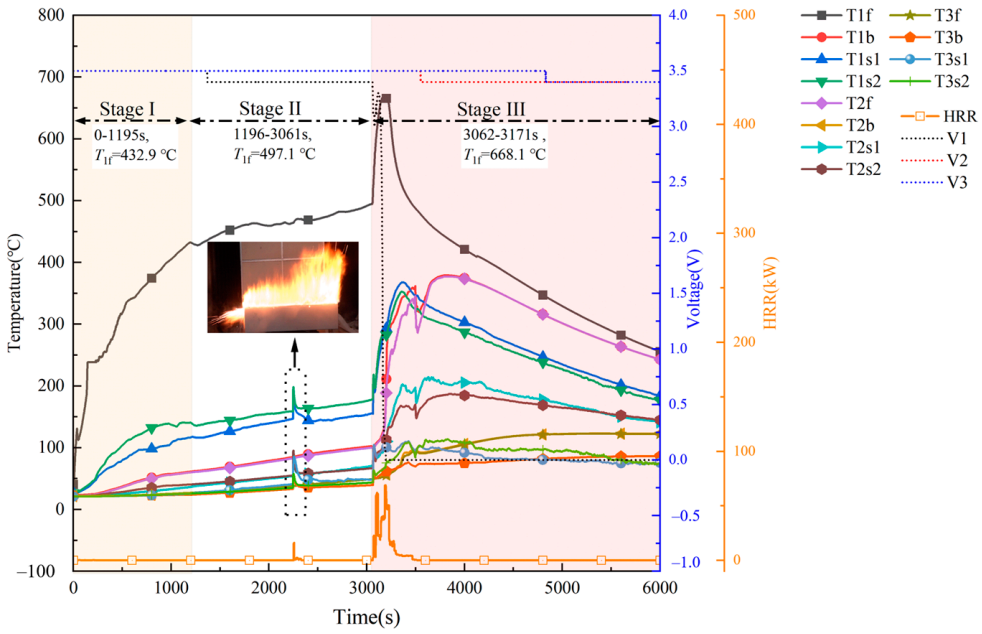


Figure 5. Curves of thermal runaway temperature, voltage, and heat release rate for lithium-ion battery packs with no fire suppression measures.

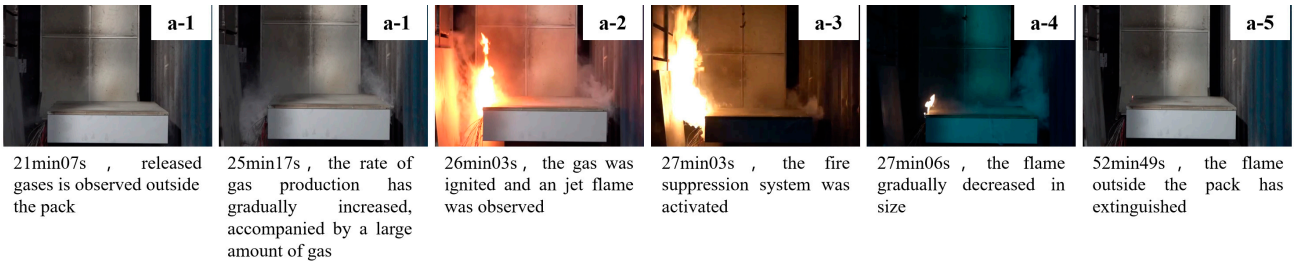
Stage III: From 3062 to 3171 s, thermal runaway occurs as the battery temperature rises rapidly. And T1f peaks at 668.1 °C at 3171 s. Subsequently, Battery 1# enters the natural cooling phase, while Batteries 2# and 3# continue to rise in temperature under the influence of intense heat from Battery 1#. The voltages V2 and V3 experience slight drops at 3549 s and 4825 s, respectively. At 3495 s, the safety valve of Battery 2# breaks, causing a partial temperature decline. However, no thermal runaway propagation ultimately occurs.

In previous studies, thermal runaway behavior was divided into four or five stages associated with the typical characteristic behavior and temperature variation, such as self-heating, safety venting, voltage drop, thermal runaway and cooling [18,19]. In the confined space experiments, the self-heating stages are hardly captured by the thermocouples and ignition stages were strongly coupled with deflagration events. Thus, the observations were consolidated into a pragmatic three stage model that captures the key transitions under our test conditions.

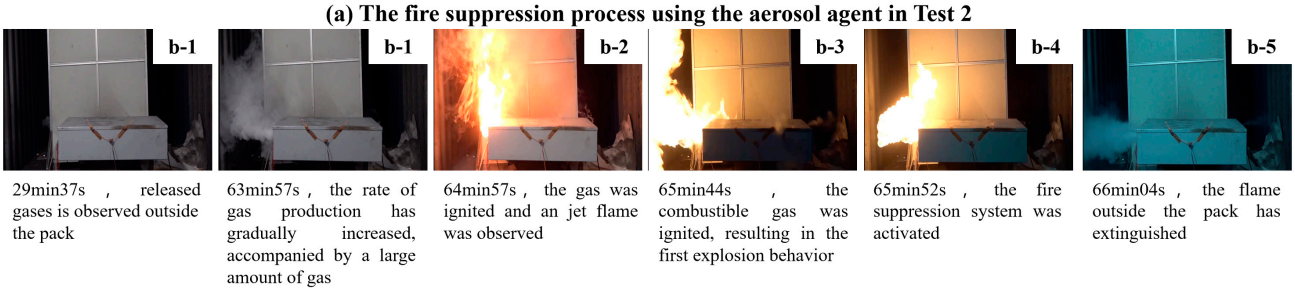
3.1. Open Flame Suppression Capability

Figure 6 illustrates the fire suppression performance of various fire extinguishing agents for battery packs. In this experiment, 30 g of aerosol was employed and could provide effective protection over an area of 0.3 m^3. Figure 6(a-1)–(a-6) demonstrate the fire suppression effects of the aerosol agent. As shown in Figure 6(a-4), the aerosol instantly released a substantial volume of gas at 1623 s, triggering a distinct jet flame outside the pack driven by the gas flow. Subsequently, the flame rapidly contracted within 3 s under the aerosol's action. However, the aerosol agent failed to completely extinguish the flame, with minor visible flames persisting until 3169 s before gradually disappearing. These results confirm the significant fire suppression efficacy for lithium-ion batteries in confined spaces using an aerosol. Nevertheless, given the battery's re-ignition tendency and prolonged thermal runaway gas generation, the single-action suppression of the aerosol

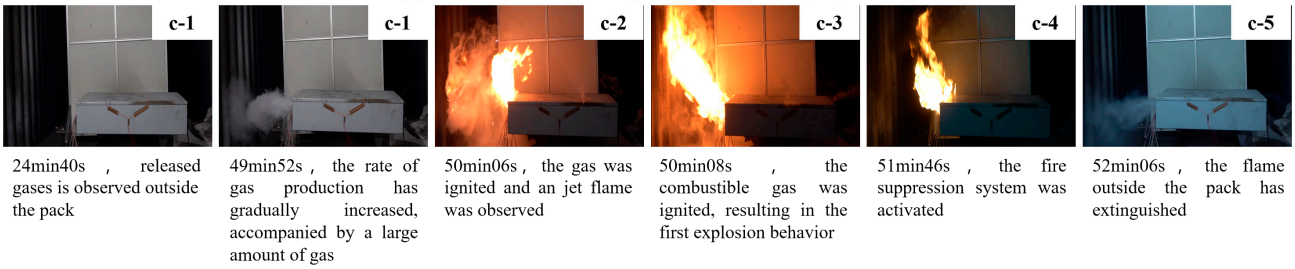
design requires greater consideration. Additionally, the experiment reveals that high-temperature heat sources in battery systems can lead to explosive combustion upon gas accumulation from thermal runaway. Therefore, energy storage battery systems should incorporate multi-jet fire suppression designs.



(a) The fire suppression process using the aerosol agent in Test 2



(b) The fire suppression process using the heptafluoropropane agent in Test 3



(c) The fire suppression process using the perfluorohexone agent in Test 4

Figure 6. Fire suppression behavior of different fire extinguishing agents in lithium-ion battery packs.

Figure 6b,c illustrate the fire suppression effects of heptafluoropropane and perfluorohexaneone on battery packs, respectively. As shown in Figure 6(b-5), a large volume of combustible gas mixed with the fire extinguishing agent is discharged through the pressure relief vent under airflow pressure after the activation of the heptafluoropropane fire suppression system. The initial flame exhibits significant intensification. However, the extinguishing agent gradually becomes dominant in the discharged gas as its concentration increases, ultimately extinguishing the flame. The fire suppression mechanism of perfluorohexaneone is analogous to that of heptafluoropropane. In this study, both agents effectively suppressed the battery flame. The heptafluoropropane system achieved complete flame extinction from activation to external flame suppression within 12 s, whereas perfluorohexaneone required 20 s.

3.2. Cooling Capacity

The temperature and voltage variations in Battery 1# in different testing conditions are shown in Figure 7. The results reveal significant differences in the cooling processes with the use of various fire extinguishing agents. As shown in Figure 7b, the aerosol rapidly covers the fire source area at the injection instant, causing a brief drop in the battery surface temperature. However, no pronounced temperature decline is observed due to its single-release nature and lack of sustained cooling capacity. Figure 7c demonstrates that the front temperature drops sharply from a peak of 508 °C to 361 °C within a short time after

the activation of the heptafluoropropane fire suppression system, representing a 147 °C reduction, with the side temperature also decreasing by 152 °C. Conversely, the temperature of the back surface continues to rise, primarily because heptafluoropropane is released in a gaseous form with a high flow velocity, carrying substantial heat away upon contact with the battery surface. Additionally, a secondary detonation is observed at approximately 48 s after the initial combustion in the relatively enclosed battery space, triggering a minor secondary temperature spike in the back surface. Following the release of perfluorohexanone, the battery's temperature trajectory mirrors that of the heptafluoropropane system but with superior cooling efficacy. The front surface temperature decreases from 626 °C to 396 °C, which is a reduction of 230 °C. Moreover, the side surface temperature rebounded to only 166 °C after the action of perfluorohexaneone. This demonstrates that perfluorohexaneone maintains a relatively low battery surface temperature post-extinction, exhibiting strong thermal absorption and heat conduction suppression capabilities.

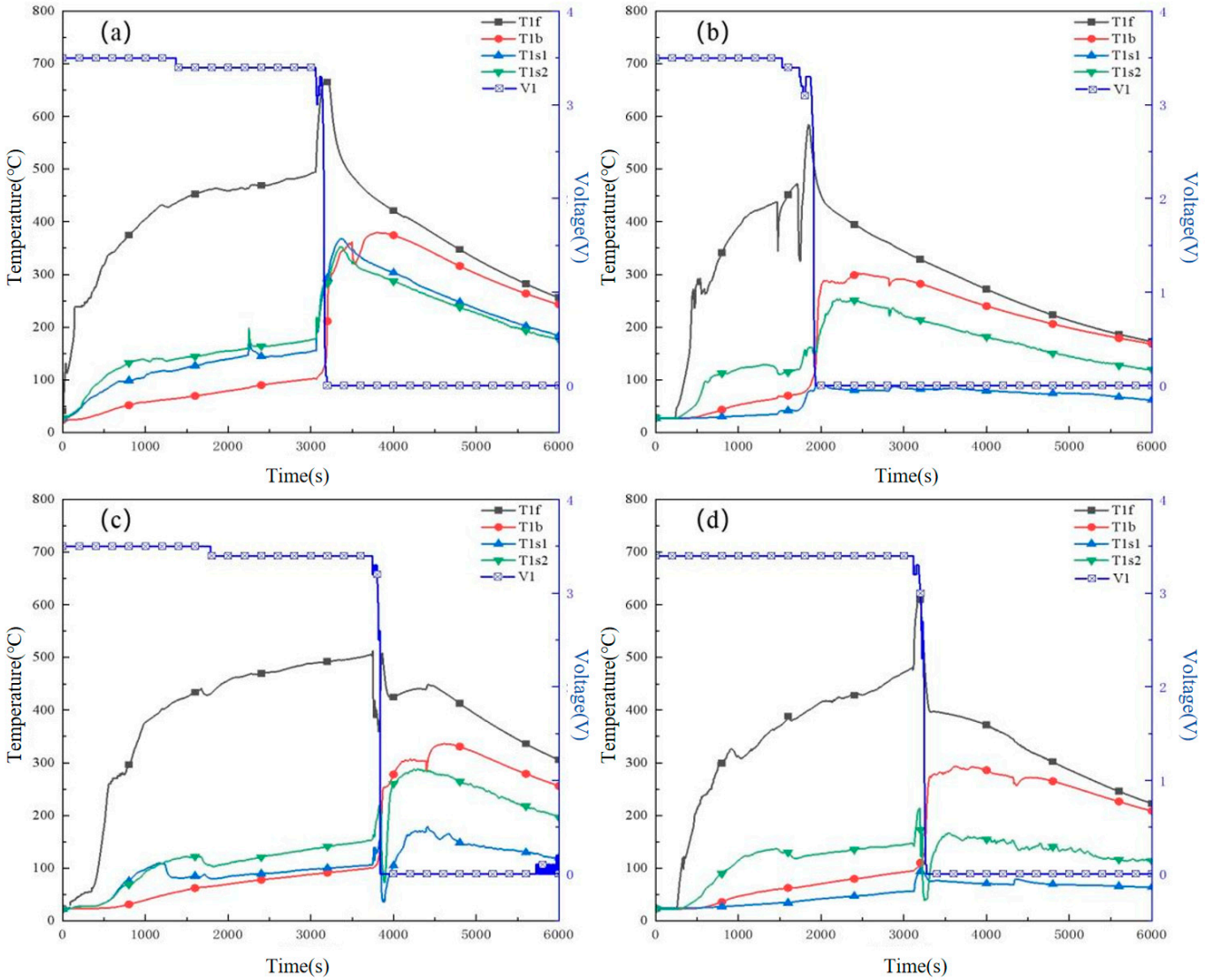


Figure 7. Surface temperature and voltage variation curves of Battery 1#. (**a**) Test 1; (**b**) Test 2; (**c**) Test 3; (**d**) Test 4.

The results demonstrate that heptafluoropropane and perfluorohexaneone outperform aerosols in both cooling efficiency and temperature maintenance. This superiority primarily stems from the distinct physical properties of these fire extinguishing agents. Heptafluo-

ropropane and perfluorohexaneone possess a high latent heat of vaporization, enabling them to absorb substantial heat during phase transitions and thus achieve the effective cooling of the battery during thermal runaway. In contrast, perfluorohexaneone can be atomized in liquid form and exhibits adhesion capabilities to contact surfaces, enabling the prolonged suppression of temperature increases. However, all three agents exert their fire-extinguishing effects through environmental coverage, resulting in limited temperature suppression capacity for adjacent battery surfaces.

Furthermore, voltage behavior varies across different thermal runaway stages of the battery, yet all exhibit a gradual decay trend only after the safety valve has operated for a period. And the battery rapidly enters a severe thermal runaway state when the voltage plummets to 0 V. This phenomenon underscores the critical importance of monitoring trace amounts of characteristic gases following safety venting during fire warning processes in energy storage systems.

With the purpose of better investigating the cooling capacity of various agent on thermal runaway behavior. The maximum temperature drop of front surface (ΔT_{max}), average cooling rate within 30 s after the initiation of extinguishing measures (CR_{avg}) as well the rebound temperature in 120 s ($T_{rebound}$) are analyzed as shown in Table 4.

Table 4. Cooling capacity of Battery 1#.

Metrics	Test 1	Test 2	Test 3	Test 4
Maximum temperature drop of front surface (°C)	/	28	147	230
Average cooling rate (°C/s)	/	0.9	4.9	7.7
Rebound temperature in 120 s(°C)	/	573	412	354

The heat release rate (HRR) was directly measured by the 10 MW calorimetry in full-scale fire simulation platform, which can be calculated using oxygen consumption calorimetry, based on the principle that the net heat released is proportional to the mass of oxygen consumed. In addition, the total heat release (THR) was obtained by integrating the HRR over time. Figure 8 shows the heat release rate and heat generation curves under various test conditions. It is evident that the battery combustion state in confined spaces exhibits significant uncertainty. The heat release rate of individual cells remains consistently above 47.8 kW after the occurrence of an open flame. The extinguishing agents cause a notable suppression of the heat generated from combustion behavior. Additionally, to reach target batteries, perfluorohexane requires a longer transit time through pipelines, resulting in a longer combustion duration compared to heptafluoropropane and aerosol products. The inhibitory effect of perfluorohexane on battery heat generation is relatively weak in this study. In practical applications, enhancing perfluorohexane's efficacy through pressure storage or increased pump system pressure could improve fire suppression performance. And we will improve the cooling capacity of the fire extinguishing medium by optimizing the firefighting strategy in our next work.

3.3. Suppression Capability for Thermal Diffusion

In lithium-ion battery energy storage systems, thermal runaway in individual batteries can trigger a chain reaction and lead to severe combustion or even explosions if the heat transfer process is not effectively suppressed. Consequently, the suppression capability of thermal diffusion serves as a key metric for evaluating the fire prevention efficacy of fire extinguishing agents in battery packs. The cooling efficiency for Battery 2# with different fire extinguishing agents and their effectiveness at inhibiting the propagation of thermal runaway are illustrated in Figure 9.

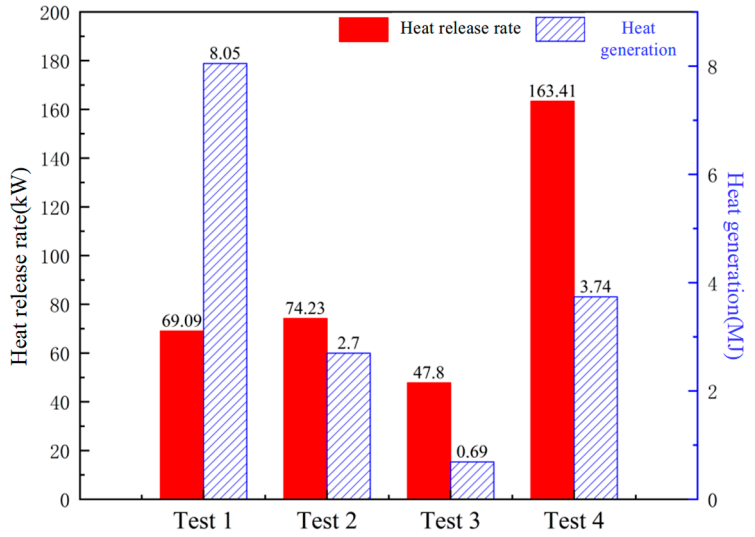


Figure 8. Test data of heat release rate and heat generation.

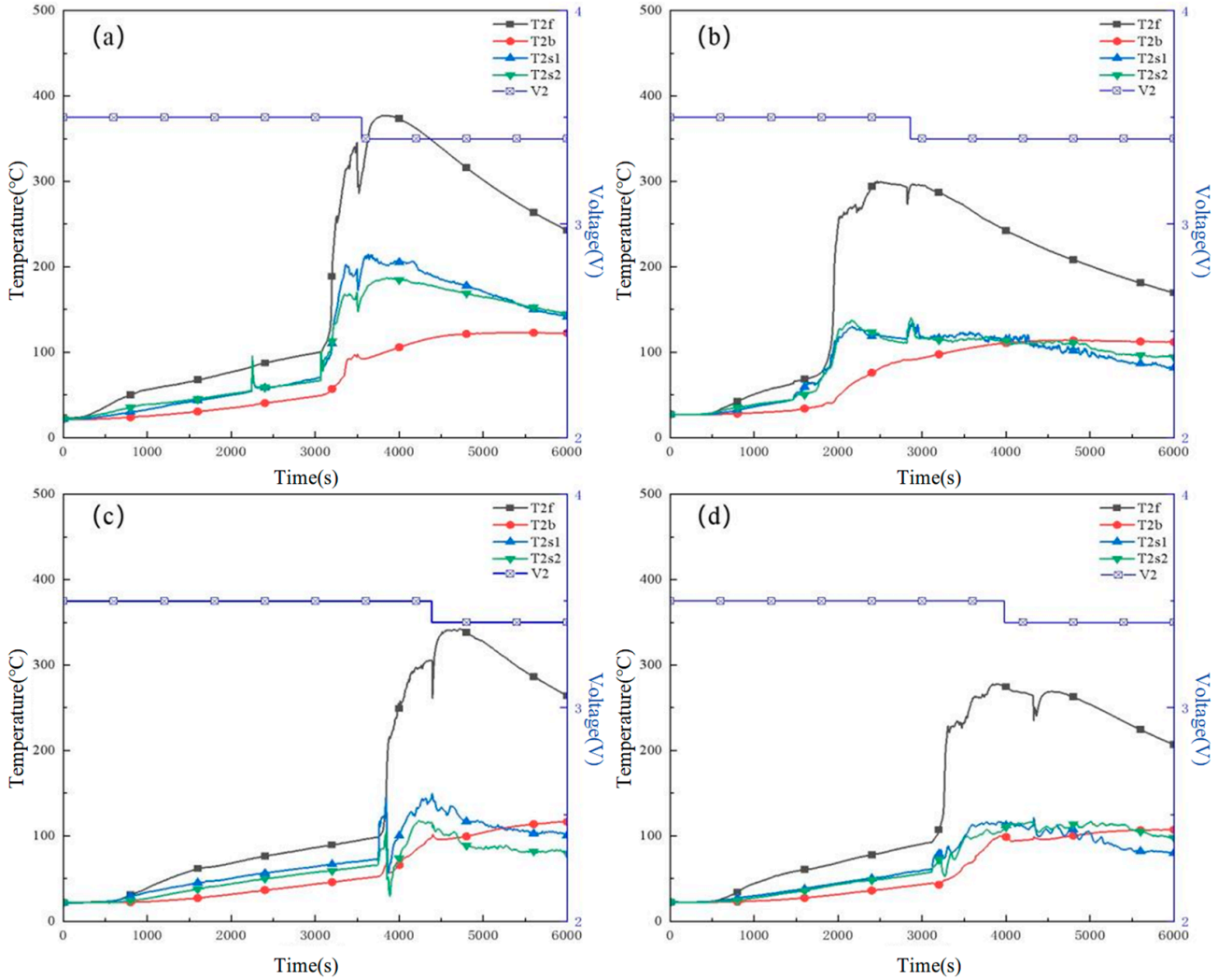


Figure 9. Surface temperature and voltage variation curves of Battery 2#. (**a**) Test 1; (**b**) Test 2; (**c**) Test 3; (**d**) Test 4.

Table 5 shows the temperature drop of the front surface of Battery 2# at 500 s, 1000 s, 2000 s, and 3000 s after reaching its peak temperature. It is evident that this cooling trend differs

significantly from that of Battery 1#. However, the fire extinguishing agent cannot directly reach the adjacent cells of Battery 2# due to the shielding effect of Battery 1#; therefore, there is a persistent heating effect of the triggered battery on neighboring cells.

Table 5. Temperature decrease (°C).

Time	Test 2	Test 3	Test 4
500 s	25	4	17
1000 s	64	25	52
2000 s	122	78	103
3000 s	168	114	141

Figure 10 illustrates the fitting of the cooling curve for Battery 2#. It is evident that the application of fire extinguishing agents has a minimal effect on blocking the heat transfer between adjacent batteries. Moreover, the cooling efficiency of Battery 2# under specific conditions decreases slightly after the application of the fire extinguishing agent.

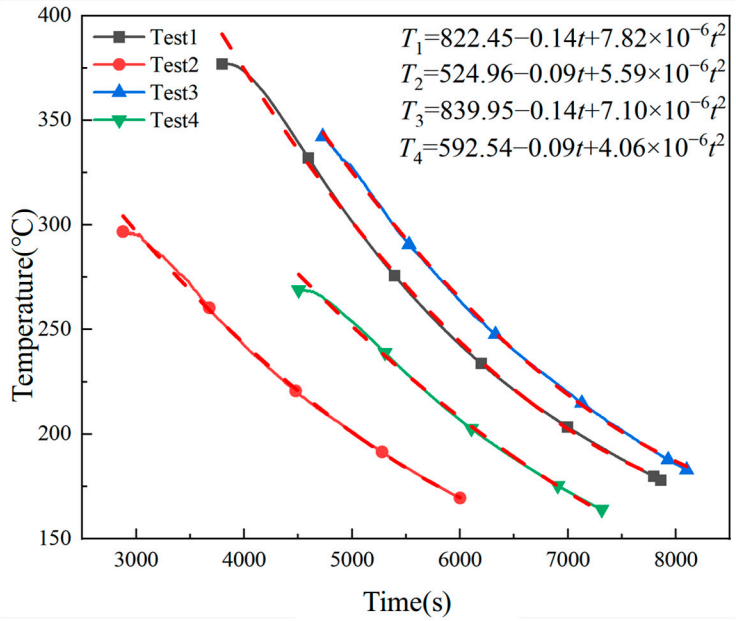


Figure 10. The fitting of the cooling curve for Battery 2#.

As shown in Table 6, the peak temperatures across different surfaces of Battery 2# demonstrate that the application of fire extinguishing agents could effectively dissipate heat generated from the triggered battery. Furthermore, the different extinguishing agents exhibited significantly varying efficacy in suppressing thermal runaway propagation within the lithium-ion battery pack. In the test without an extinguishing agent, all measurement points on Battery 2# recorded the highest peak temperatures among the four tests (front surface: 377 °C; side surfaces: 214 °C and 187 °C; back surface: 126 °C). The perfluorohexane agent demonstrated the most effective thermal diffusion suppression, with its front surface temperature (277 °C) reduced by 100 °C, while its side surface temperatures (116 °C, 113 °C) and back surface temperature (107 °C) were the lowest among all tests. This was attributed to its liquid-phase adhesion properties that maintained continuous cooling on the battery surface, inhibiting the multidirectional heat transfer process. In addition, the front surface temperature decreased by 78 °C under the aerosol application, while side surface temperatures dropped by 28–35%, though back surface temperatures remained elevated. The heptafluoropropane agent effectively controlled side surface temperatures

(118–150 °C) but exhibited an insufficient capability to suppress thermal transfer on the front surface. Temperature distributions across all tests followed a gradient pattern of front surface > side surface > back surface, with a maximum temperature gradient of 32 °C between side surfaces, reflecting an uneven agent distribution within the container. Therefore, fire protection designs for energy storage systems should optimize nozzle placement to ensure the uniform coverage of critical heat transfer pathways across the battery pack.

Table 6. Peak temperature (°C).

Thermocouple	Test 1	Test 2	Test 3	Test 4
T2f	377	299	342	277
T2b	126	114	116	107
T2s1	214	140	150	116
T2s2	187	134	118	113

Furthermore, suppression capability for thermal diffusion can be evaluated by three quantitative metrics. The peak temperature reduction ratio (R_{decrease}) can be calculated as follows:

$$R_{decrease} = \left(T_{\text{no-agent}} - T_{\text{agent}}\right) / T_{\text{no-agent}} \times 100\% \quad (1)$$

where $T_{\text{no-agent}}$ is the peak temperature in Test 1 without agent; T_{agent} is the peak temperature in other tests using agent.

In addition, the interval time (Δt) between the peak temperature of Battery 1# and the onset of a sustained (>10 °C above ambient) temperature rise on the front surface of Battery 2# is also compared. And the difference between the front and back surface temperatures of Battery 2# (ΔT_{grad}) are also shown in Table 7.

Table 7. Suppression capability for Battery 2#.

Metrics	Test 1	Test 2	Test 3	Test 4
R_{decrease} (%)	/	20.7	9.3	26.5
Δt (s)	0	78	45	112
ΔT_{grad} (°C)	251	185	226	170

These metrics clearly demonstrate that perfluorohexanone offers the best overall performance in both cooling efficiency and thermal propagation suppression, while heptafluoropropane provides a rapid initial cooling but weaker sustained suppression. The aerosol shows only marginal cooling and intermediate propagation delay.

4. Conclusions

This study comparatively analyzed the suppression performance of three typical extinguishing agents (aerosol, heptafluoropropane, and perfluorohexanone) on lithium-ion phosphate battery packs by conducting fire suppression experiments in a confined space within an energy storage system. The performance was systematically evaluated considering multiple aspects, including open flame extinguishing ability, cooling efficiency, the heat release rate, and thermal propagation suppression capability. The main conclusions are as follows.

In the test without an extinguishing agent, the thermal runaway process of a lithium-ion battery in a confined space exhibits distinct stages: a heating-induced stage, a thermal runaway evolution stage, and a thermal runaway occurrence stage. In the confined space, the combustible gases released and rapidly mixed with air after safety venting, leading to multiple deflagration events under continuous heat accumulation. And the peak heat

release rate reached 69.09 kW, with a total heat release of 8.05 MJ. The voltage response lagged behind the gas and smoke release, indicating that characteristic gas monitoring is more time-sensitive than voltage monitoring for safety warnings in energy storage systems.

Regarding the suppression capability for open flames, both heptafluoropropane and perfluorohexanone effectively extinguished the battery jet flames, with extinguishing times of 12 s and 20 s, respectively, and the aerosol agent failed to achieve complete extinguishment due to re-ignition, although it did cause rapid flame contraction. Therefore, fire suppression designs for energy storage battery systems should prioritize multiple extinguishing capabilities to address the prolonged gas release from the battery thermal runaway process.

A comprehensive comparison of the three agents demonstrates that perfluorohexanone exhibits outstanding performance in terms of open flame extinguishment, cooling efficiency, and thermal propagation suppression. Its liquid-phase adhesion properties provide long-lasting cooling effects, making it suitable for fire prevention and control in energy storage battery packs. Heptafluoropropane offers a fast extinguishing speed and significant gas-phase dispersion, making it suitable as a fast-response extinguishing medium. Although the aerosol is low-cost and rapidly suppresses open flames, it carries a risk of re-ignition and has limited thermal propagation suppression capability, requiring a multi-extinguishing design.

In this study, the application of three extinguishing agents demonstrated the limited prevention capability of heat transfer between adjacent batteries. Therefore, fire protection designs for lithium-ion battery energy storage systems should adopt a composite fire suppression strategy combining rapid flame extinguishment and long-lasting cooling. The nozzle placement should be optimized to ensure the uniform coverage of the agents over the key heat transfer paths of the battery pack. Additionally, the fire suppression system should be coordinated with the ventilation and explosion venting system to effectively dilute and vent flammable gases while suppressing the fire, reducing the risk of deflagration.

Author Contributions: Experiment, Y.J.; validation, S.H. and A.T.; formal analysis, C.S. and L.Z.; writing—original draft preparation, Y.J. and H.L.; writing—review and editing, H.L.; project administration, Y.J. and A.T.; funding acquisition, A.T. All authors have read and agreed to the published version of the manuscript.

Funding: This work was supported by the Research Project on Fire Safety of Electrochemical Energy Storage Systems and the National Natural Science Foundation of China (52404259).

Data Availability Statement: The data presented in this study are available on request from the corresponding author. The data cannot be made publicly available due to confidentiality reasons.

Conflicts of Interest: Authors Yanbo Jia, Chaohui Shi, Lei Zhang, An Tao, and Sen Hu are employed by the company Power China HuaDong Engineering Corporation Limited. The remaining author declares that the research was conducted in the absence of any commercial or financial relationships that could be construed as a potential conflict of interest.

References

1. Kong, L.; Li, C.; Jiang, J.; Pecht, M. Li-Ion Battery Fire Hazards and Safety Strategies. *Energies* **2018**, *11*, 2191. [CrossRef]
2. Goldsmith, V. Introduction to grid-scale battery energy storage system concepts and fire hazards. *Process Saf. Prog.* **2024**, *43*, 357–363.
3. Wang, H.; Xu, H.; Zhang, Z.; Wang, Q.; Jin, C.; Wu, C.; Xu, C.; Hao, J.; Sun, L.; Du, Z. Fire and explosion characteristics of vent gas from lithium-ion batteries after thermal runaway: A comparative study. *eTransportation* **2022**, *13*, 100190. [CrossRef]
4. Larsson, F.; Bertilsson, S.; Furlani, M.; Albinsson, I.; Mellander, B.-E. Gas explosions and thermal runaways during external heating abuse of commercial lithium-ion graphite-$LiCoO_2$ cells at different levels of ageing. *J. Power Sources* **2018**, *373*, 220–231.

5. Wei, G.; Huang, R.; Zhang, G.; Jiang, B.; Zhu, J.; Guo, Y.; Han, G.; Wei, X.; Dai, H. A comprehensive insight into the thermal runaway issues in the view of lithium-ion battery intrinsic safety performance and venting gas explosion hazards. *Appl. Energy* **2023**, *349*, 121651. [CrossRef]
6. Xie, W.; Zhang, L. Experimental study on thermal runaway and venting gas explosion hazards in prismatic lithium-ion batteries at different states of charge. *Process Saf. Environ. Prot.* **2025**, *198*, 107118. [CrossRef]
7. Chen, M.; Dongxu, O.; Liu, J.; Wang, J. Investigation on thermal and fire propagation behaviors of multiple lithium-ion batteries within the package. *Appl. Therm. Eng.* **2019**, *157*, 113750. [CrossRef]
8. Gagnon, L.; Zeng, D.; Barlow, R.S.; Wang, Y. Detailed measurements of thermal runaway propagation and fire spread for Li-ion battery multi-module setup. *J. Energy Storage* **2025**, *134*, 118292.
9. Wang, Q.; Wang, H.; Xu, C.; Jin, C.; Wang, S.; Xu, L.; Ouyang, J.; Feng, X. Multidimensional fire propagation of lithium-ion phosphate batteries for energy storage. *eTransportation* **2024**, *20*, 100328. [CrossRef]
10. Wang, Z.; Xie, R.; Song, Y.; Shi, B.; Li, J.; Wang, W.; Hou, Y. Fire behavior and hazard propagation in a lithium-ion battery energy storage cabin under microgravity environments. *J. Energy Storage* **2026**, *152*, 120755. [CrossRef]
11. Meng, X.; Yang, K.; Zhang, M.; Gao, F.; Liu, Y.; Duan, Q.; Wang, Q. Experimental study on combustion behavior and fire extinguishing of lithium iron phosphate battery. *J. Energy Storage* **2020**, *30*, 101532. [CrossRef]
12. Xu, J.; Guo, P.; Duan, Q.; Yu, X.; Zhang, L.; Liu, Y.; Wang, Q. Experimental study of the effectiveness of three kinds of extinguishing agents on suppressing lithium-ion battery fires. *Appl. Therm. Eng.* **2020**, *171*, 115076. [CrossRef]
13. Yuan, S.; Chang, C.; Yan, S.; Zhou, P.; Qian, X.; Yuan, M.; Liu, K. A review of fire-extinguishing agent on suppressing lithium-ion batteries fire. *J. Energy Chem.* **2021**, *62*, 262–280.
14. Zhang, L.; Jin, K.; Sun, J.; Wang, Q. A review of fire-extinguishing agents and fire suppression strategies for lithium-ion batteries fire. *Fire Technol.* **2024**, *60*, 817–858.
15. Mao, Y.; Chen, Y.; Chen, M. Review of flame behavior and its suppression during thermal runaway in lithium-ion batteries. *Batteries* **2024**, *10*, 307. [CrossRef]
16. *GB36276*; Lithium-Ion Battery for Power Energy Storage. China Electricity Council: Beijing, China, 2023.
17. *GB50370*; Code for Design of Gas Fire Extinguishing Systems. Tianjin Fire Science and Technology Research Institute of MEM: Tianjin, China, 2005.
18. Li, H.; Duan, Q.; Zhao, C.; Huang, Z.; Wang, Q. Experimental investigation on the thermal runaway and its propagation in the large format battery module with $Li(Ni_{1/3}Co_{1/3}Mn_{1/3})O_2$ as cathode. *J. Hazard. Mater.* **2019**, *375*, 241–254. [PubMed]
19. Feng, X.; Fang, M.; He, X.; Ouyang, M.; Lu, L.; Wang, H.; Zhang, M. Thermal runaway features of large format prismatic lithium ion battery using extended volume accelerating rate calorimetry. *J. Power Sources* **2014**, *255*, 294–301. [CrossRef]

Disclaimer/Publisher's Note: The statements, opinions and data contained in all publications are solely those of the individual author(s) and contributor(s) and not of MDPI and/or the editor(s). MDPI and/or the editor(s) disclaim responsibility for any injury to people or property resulting from any ideas, methods, instructions or products referred to in the content.